SIZING OF PNEUMATIC DRIVES UNDER ENERGY EFFICIENCY ASPECTS

Matthias Doll[1]*, Rüdiger Neumann[1], Wolfgang Gauchel[1]

[1]*Festo SE & Co. KG, Ruiter Str. 82, 73734 Esslingen*

* Corresponding author: Tel.: +49 711 347-57380; E-mail address: matthias.doll@festo.com

ABSTRACT

The correct sizing of pneumatic drives plays a central role when it comes to energy efficiency. While there are simple design formulas for force-based tasks such as pressing or clamping in order to size the drive efficiently, there is no such easy methodology for motion tasks.

Up to now, the sizing of pneumatic drives has mainly been experience-based or simulation-based. A tool from Festo [1] now enables formula-based sizing without simulation, which directly provides the optimum piston diameter and other components. The approach behind this is based on the natural frequency of the pneumatic drive.

The main drawback of this method is that it is only applicable for horizontal installation positions. Based on more recent findings (which arose in a joint project with the TU Dresden [2]) and based on numerous simulations and measurements, this formula has now been extended so that it can also be used with external forces and thus also for a vertical installation position.

Keywords: pneumatic drives, energy efficiency, sizing

1. INTRODUCTION

Pneumatic drives are used in numerous applications in industrial machines. They are known for their simplicity, robustness, high power density, compact design and high forces. They are controlled by a switching valve in combination with exhaust air throttles to adjust the speed. The energy consumption only depends on the internal volume of the cylinder. In the age of global warming, the efficiency of drive systems becomes increasingly important.

The simplest way to increase the efficiency of the drives is the sizing of the cylinder in order to reduce its volume. **Dimensioning** generally describes the process of assigning system components (such as cylinders, valves, etc.) to a given application. In addition to the application parameters such as stroke, force, transition time and moving mass, several additional factors like end position energy, vibrations, requirements on the motion profile (velocity, acceleration), guide load, lateral forces and special requirements like ATEX or LABS-free etc. are important.

Once a cylinder has been found that can solve the application, additional requirements can be realized by selecting a suitable series and additional options. However, even the sizing process of the required piston diameter is not trivial for many applications and therefore often results in oversized drive systems. Other reasons for oversized drive systems include:

- Safety factors and robustness issues
- Storage costs for spare parts (reducing variants, one size for all applications)
- Usage of cylinders as construction elements (mechanical stability)

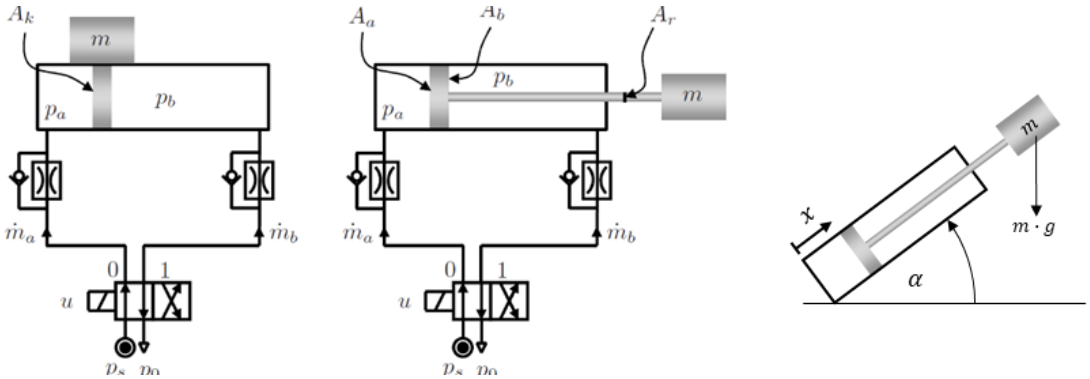

Figure 1: Standard pneumatic system using a rodless cylinder (*left*) and cylinder with rod (*middle*), standard switching valves and exhaust flow throttles for speed adjustment. *Right:* orientation.

In principle, a distinction must be made in the **dimensioning** between force and movement tasks.

Force tasks are applications in which a force plays the central role within the process, e.g. in pressing processes, rolling, joining, etc. They are relatively easy to design, as the specified force F is in a direct, algebraic relationship with the piston area A_k and the pressure difference Δp and therefore can be used for calculating the effective area:

$$F = A_k \cdot \Delta p. \tag{1}$$

Motion tasks are applications that require a movement within a specified time T_f. They are typically described by the moving mass, stroke, transition time, and a pressure level. For motion tasks an easy relationship as in (1) cannot be represented. In contrast to controlled electric drives, the movement profile and therefore the acceleration profile cannot be specified directly. Instead, it results from the selected system components and the throttle values. The aim of the design here is to achieve a defined transition time. Differential equations are used to describe the system behaviour [3]. The determination of the transition time as well as the design process itself is therefore often simulation-based in combination with a variation of the throttle positions and the drive size. An important aspect in the design for motion tasks is the **kinetic energy** in end position, as this must be below a specified limit so that the drive can be operated permanently without destruction. This boundary condition determines the feasibility of an application with a selected system. Mixed forms of force and movement tasks are also frequently used.

The **energy consumption** of a pneumatic actuator can be calculated directly from the air consumption [4]. In standard operation (switching valve + exhaust air throttling), it depends solely on the selected size (and the dead volume) and is independent of the throttle position and the resulting transition time. This makes the **sizing** particularly important for reducing energy consumption. Ultimately, it leads to the central question:

"What is the smallest possible cylinder to fulfil the motion task?"

1.1. Starting point

We consider standard pneumatic drives consisting of a cylinder with exhaust air throttles and an adjustable pneumatic cushioning system and a switching valve as shown in **Figure 1**. The design methodology focuses on motion tasks (with additional force requirement), i.e. on the sizing of the system components for a specified application given by: mass, stroke, transition time, supply pressure, external force and a permissible end position behaviour (compliance with the maximum permissible residual energy). The focus here is on energy efficiency, so that a design methodology for medium to large drives is required, as small or short stroke drives require only little energy in absolute terms.

2. STATE OF THE ART

In addition to simulation-based design methods, there are efforts to map the non-linear and complex processes of the dynamic model in algebraic formulas for a sizing purpose. Even if the force and acceleration profiles result from the application and can only be specified in a highly simplified form, there are a number of methods that attempt to do just that. These include force equilibrium method [5], minimum cylinder [3], exergy equilibrium method [6], operating point analysis [7].

In principle, a distinction can be made between two different assumptions regarding the motion profile: constant acceleration and constant speed.

2.1. Assumption of constant acceleration

The following approaches fall into this category: force equilibrium method [5], exergy equilibrium method [6], minimum cylinder [3]. The common idea behind those methods is that if we search for the smallest cylinder which fulfils the given application (without considering the kinetic energy at end stop) we must apply the maximum acceleration all the time. The result is that the speed increases and reaches its maximum at the end stop. The above-mentioned methods differ in their physical derivation but lead to very similar results and equations. In [5] and [6] constant friction forces are assumed for a cylinder whose diameter is not known yet. Therefore, iterations may be necessary to adjust the friction force in dependence on the chosen piston diameter. In [3] the constant friction is replaced by a friction model using Coulomb and viscous friction. The result is similar than in the other equations, but due to the viscous friction the velocity will reach a constant value if the stroke length is long enough.

2.2. Assumption of constant velocity

A constant velocity can also be directly specified in the known methods: force equilibrium method [5], exergy equilibrium method [6] and operating point analysis [7]. As shown in [5], the results are very similar but not equal.

Both the approaches with constant acceleration and constant velocity have the same drawback: the velocity at stroke end and therefore the kinetic energy is not taken into account. This means that the applicability of those methods seems to be restricted - but also suitable - only for short stroke cylinders with low payloads. For longer strokes (and therefore higher velocities) shock absorbers have to be used. Short stroke cylinders with low payload however will not need much energy, s.th. energy efficiency considerations are less important.

2.3. Assumption of a damped system behaviour at stroke end

In contradiction to the previous mentioned methods no direct assumption on the trajectory is made. Only the assumption of realising a velocity at end stop which yields in a kinetic energy value below the given limit. The only approach using this assumption is published in [8,3] and makes use of the eigenfrequency of the pneumatic system. In [5] some extensions of the eigenfrequency approach were made: an additional external spring force was integrated, a polytropic change of state was assumed, and both cylinder chambers were treated independently. In [9] a similar formula – the dimensionless mass – is derived by similarity considerations and is used for a special control strategy.

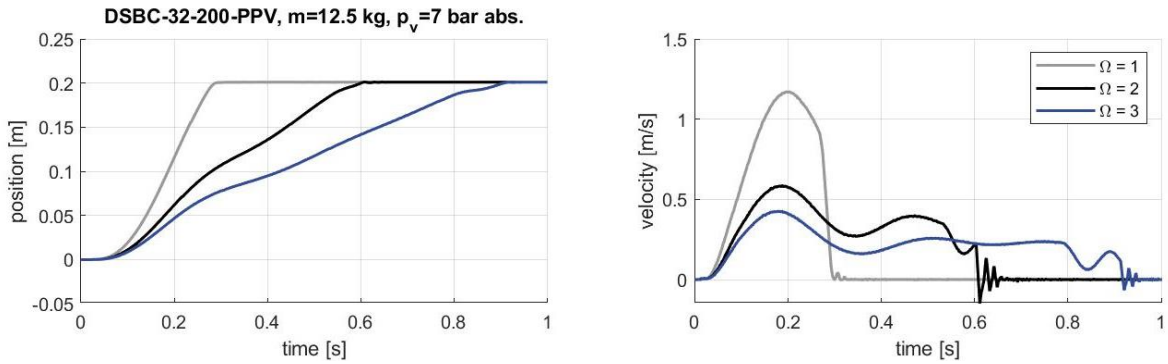

Figure 2: Measurements of the dynamic behaviour of a cylinder in dependence on the exhaust flow throttle and the resulting PFR values.

3. THE PNEUMATIC FREQUENCY RATIO (PFR)

The pneumatic frequency ratio (PFR) was published in [8,3] and expresses the ratio of the pneumatic eigenfrequency ω_0 and the application specific frequency $\omega_f = 2\pi/T_f$ which is given by the transition time T_f. Therefore, it expresses the ratio of the speed (expressed in terms of ω) the system would be able to do (ω_0) and the speed the system achieved within the application (ω_f):

$$\Omega = \frac{\omega_0}{\omega_f} = \frac{T_f}{\pi}\sqrt{\frac{A_k p}{mL}} \tag{2}$$

This formula depends on the effective area of the cylinder A_k, the load m, the transition time T_f, the supply pressure level p and on a characteristic length L. The characteristic length L includes the stroke length l_z and an additional length l_t resulting from the dead volume: $L = l_z + l_t$. The idea behind this formula is that the PFR characterizes the system behaviour, such that all systems with the same PFR behave similar. In [8] an optimal $\Omega = 1$ is determined by evaluating simulation data of optimal movements. Optimal movements mean that it moves as fast as possible but with the restriction of having a damped system behaviour at stroke end such that the kinetic energy at the end stop does not exceed the permissible value. For those movements a PFR of $\Omega = 1$ has been determined. **Figure 2** shows the dynamic response of a system in dependence on the PFR. Optimal behaviour is achieved with $\Omega = 1$ as no oscillations at stroke end are visible in the velocity signal.

3.1. Calculation of the required piston diameter

Equation (2) can now be used for several tasks: characterizing a system by using (2) directly, calculating an optimal diameter d of a cylinder for a given application (with $A_k = \pi/4 \cdot d^2$), calculating the necessary supply pressure level and to estimate the transition time T_f for a given system. Both most important inversions are listed below:

$$d = \frac{2\pi\Omega}{T_f}\sqrt{\frac{mL}{\pi p}} \tag{3}$$

$$T_f = \pi \cdot \Omega \sqrt{\frac{mL}{A_k p}} \tag{4}$$

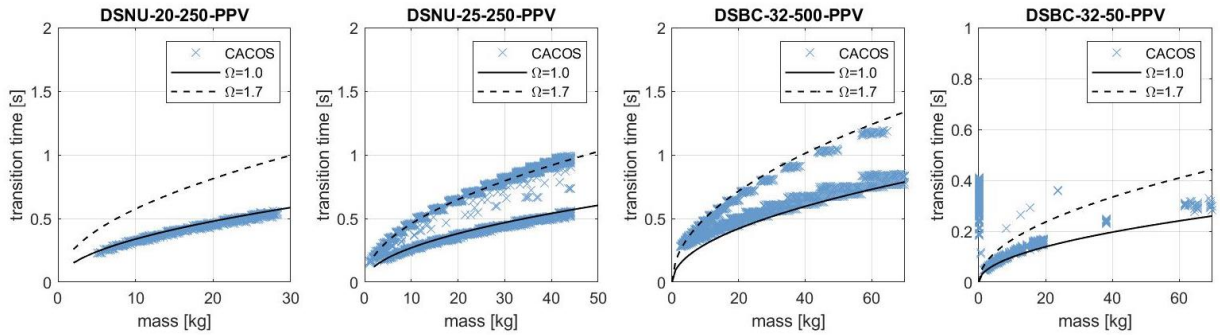

Figure 3: Approximation of the transition time using the PFR for several cylinders in horizontal orientation.

As in [8], once again we simulated a whole bunch of systems and applications by varying all the parameters (piston diameter $d \in \{20,25,32,50,80\}$ mm, stroke length $l_z \in \{50,100,200,250,500\}$ mm, pressure p, load $m \in [0,200]$ kg). Additionally, the exhaust flow throttle and the throttle of the pneumatic cushioning system (PPV) were varied in order to find a suitable combination. Useful combinations lead to a damped system behaviour which fulfil the condition for the kinetic energy at stroke end. Only those results are used afterwards, leading to optimal results (having no oscillations within the pneumatic cushioning system). The simulation study was made with CACOS (a simulation tool of Festo) and contains approximately 5 Mio. Simulations and 27.000 optimal results. **Figure 3** shows the comparison of those optimal simulations of several systems and their corresponding approximation of the transition time T_f using (4). The PFR reflects quite good the simulation results for all types of cylinders in horizontal orientation. In most the graphics there is a second optimality curve visible for a PFR of $\Omega \approx 1.7$ which can be approximated using (2) respectively (4), too.

Figure 4 shows again the results for one system (DSBC-32-200-PPV of Festo SE & Co. KG) in different orientations. Again, the PFR matches quite good for horizontal orientation, but for vertical orientation there is an obvious mismatch between the simulation result and the PFR. This is due to the gravitational forces which are not included in (2).

3.2. Calculation of the required sonic valve conductance

Once the piston diameter is specified, the sonic conductance of the valve can be calculated using a mean value of the required mass flow [8]:

$$C_v = K_C \frac{A_k L}{T_f} = K_C \cdot \pi^2 \Omega^2 \frac{mL^2}{T_f^3 p} \tag{5}$$

Thereby K_C is a constant which must be determined [8]. Concerning energy efficiency however, the valve conductance does not have a direct influence. It is important, that the sonic conductance is great enough to fulfil the required pressure dynamics of the application. Strictly speaking, (5) does not give the necessary conductance of the valve, but the necessary total conductance consisting of the valve, hose, and inlet port of the cylinder. The valve must be chosen, s.th. the overall conductance is met.

This dimensioning method is also part of the tool “Pneumatic Sizing” of Festo SE & Co. KG for an adjustable cushioning and is available online at: https://www.festo.com/x/pneumatic-sizing [1].

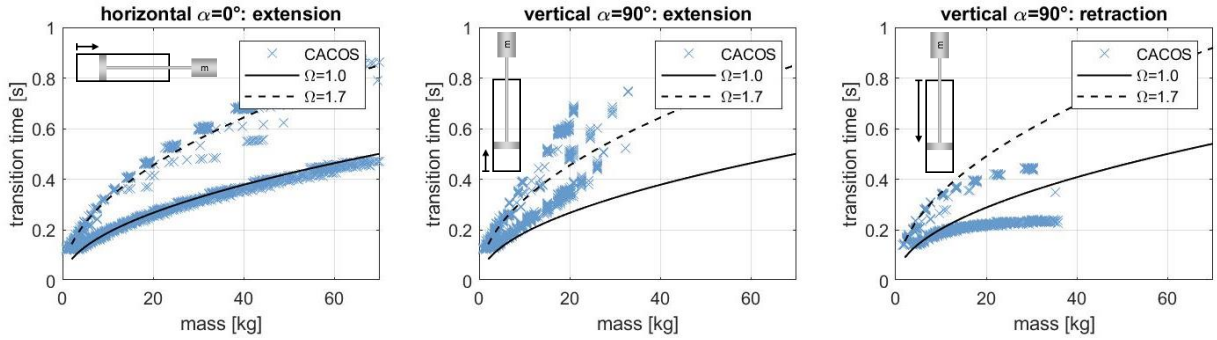

Figure 4: Approximation of the transition time using the PFR for horizontal and vertical orientation of a DSBC-32-200-PPV of Festo SE & Co. KG.

4. EXTENSION OF THE PFR FOR APPLICATIONS WITH EXTERNAL FORCES

As shown in [5] and [8], the application of PFR (2) is limited to horizontal load cases, as gravitational forces cannot be fully compensated by an adapted dimensioning of the cylinder using (2). This holds also for other external forces like forces resulting from the process e.g., for pressing or clamping and for increased friction forces due to external guidance.

Therefore, another simulative study was carried out for several systems by varying not only the load, and the throttles, but also an external force. The external force is a counter force, s.th. a positive value indicates a force against the direction of motion. **Figure 5** shows the results of all optimal solutions for a DSBC-32-200-PPV cylinder in dependence on the external forces. It shows, that for each curve of constant external force the transition times can be approximated by adjusting the PFR. As the external force increases, the transition time of an optimal movement decreases and therefore results in a higher value for Ω according to (2). This however would indicate that the system is oversized (in the sense of PFR), but due to the external force it is not the case: it is well sized because all the data points are optimal solutions. As for the PFR Ω, this should be reflected by the extended version, too. In other words: all optimal solutions should have the same value for Ω_{ext} - independent of the applied force F. The new equation for an extended PFR Ω_{ext} should also satisfy the following condition: $\Omega_{ext}(\mathrm{F} = 0) = \Omega$. The following ansatz function was used for finding an extended version of the PFR:

$$\Omega_{ext} = \Omega \cdot f(F) \tag{6}$$

The function $f(F) = \Omega_{ext}/\Omega$ is now identified using the measured values for Ω shown in **Figure 5**. For $\Omega_{ext} = 1$ it is the reciprocal of the measured Ω-values and is illustrated in **Figure 5** on the right in blue. We found out that its slope equals to: $-1/(A_k p)$, such that the searched function for extending the PFR can be stated as:

$$f(F) = 1 - K \cdot \frac{F}{A_k p} \tag{7}$$

Thereby we introduced an additional factor $K \approx 1$ for adjustments. This function equals to one when no force is applied and becomes zero for $K = 1$ and $F = A_k p$ which is the maximum force of the driving chamber. Using this function (7) and (6) the extended PFR can be stated as:

$$\Omega_{ext} = \Omega \cdot \left(1 - K \cdot \frac{F}{A_k p}\right) = \frac{T_f}{\pi} \sqrt{\frac{A_k p}{mL}} \cdot \left(1 - K \cdot \frac{F}{A_k p}\right) \tag{8}$$

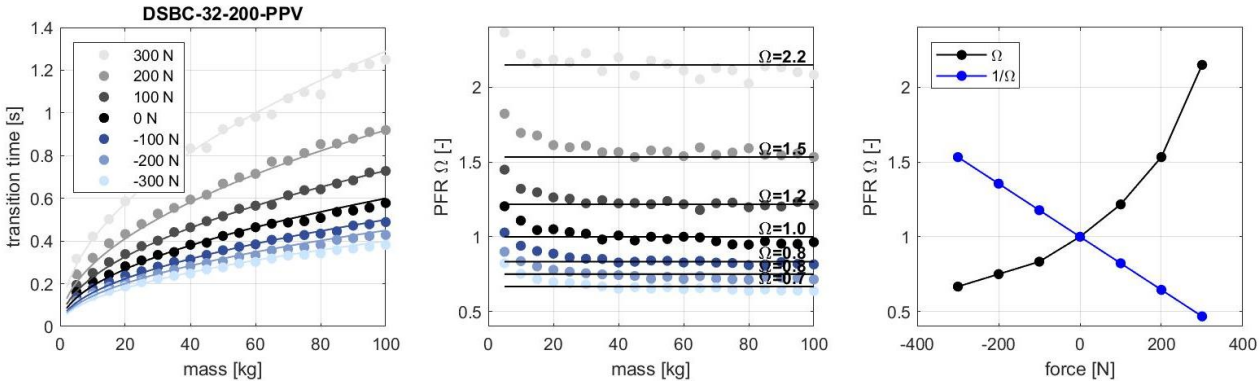

Figure 5: Simulation results (*dots*) of optimal movements in dependence of the load m and the external force F in comparison to the PFR approximation (*solid line*). *Left*: transition time, *middle*: PFR, *right*: PFR in dependence on the external force.

For $F = 0$, we get $\Omega_{ext} = \Omega$, for $F = A_k p$, we get $\Omega_{ext} = 0$. In this case, the external force equals the maximum force of the cylinder, such that it won't move. All in all, we found out, that the force F should not exceed 50% of the maximum force of the cylinder to guarantee a proper motion. As for the PFR, the extended version (8) can now be used for several purposes by inversion. Especially for dimensioning the piston diameter, the following inversion is of interest:

$$d_{ext} = \left(\Omega_{ext} + \sqrt{\Omega_{ext}^2 + 4\left(\frac{T_f}{\pi}\right)^2 \frac{KF}{mL}} \right) \Big/ \left(2T_f \sqrt{\frac{p}{4\pi \cdot m \cdot L}} \right). \tag{9}$$

For validating the simulation data, the transition time is also a useful inversion:

$$T_f = \pi \cdot \Omega_{ext} \sqrt{\frac{mL}{A_k p}} \cdot 1 \Big/ \left(1 - K \frac{F}{A_k p}\right). \tag{10}$$

Figure 6 shows again the optimal simulation data, but this time in comparison to the equations of the extended PFR (8) and (10). On the left we see that the transition times are approximated quite well by using (10). And the graph in the middle proves that all the measured transition times correspond to an extended PFR of approximately $\Omega_{ext} = 1$ independent on the external forces. There is a slight deviation for lower loads at high speed of the piston. This might be a result of viscous friction forces or of pressure losses which increase with the velocity. Additionally, **Figure 7** shows further validation data for a lower supply pressure and for other piston diameters and stroke lengths. The approximation (8) matches quite good also for these combinations.

4.1. Applications with gravitational forces

As shown in the previous section, the extended version of the PFR reflects quite good the influence of external forces. In this section we will use and test it with systems in vertical orientation. The force F needed in (8) therefore evaluates to:

$$\begin{aligned} F &= m \cdot g \cdot \sin\alpha\,, \qquad \text{for extension} \\ F &= -m \cdot g \cdot \sin\alpha\,, \qquad \text{for retraction} \end{aligned} \tag{11}$$

Thus, the applied force varies with the used mass and is also dependent on the direction of movement. **Figure 8** shows the same data set of **Figure 4** but now in comparison with the extended version of PFR. It shows that (10) now approximates the transition times quite well also in vertical orientation (α =+90°) for the extension stroke as well as for the retraction stroke.

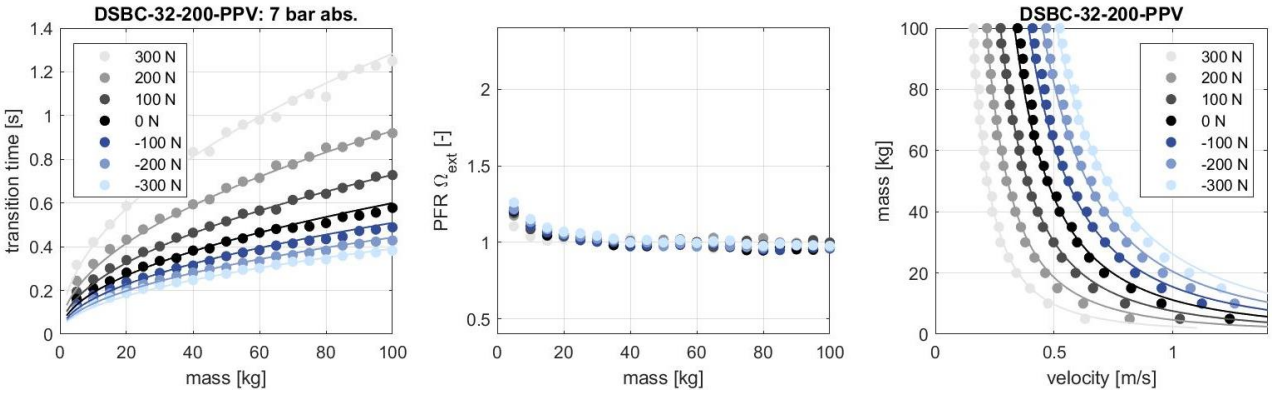

Figure 6: Simulation results (*dots*) of optimal movements in dependence of the load m and the external force F in comparison to the extended PFR approximation (*solid line*). *Left:* transition time, *middle:* extended PFR, *right:* mass-velocity diagram.

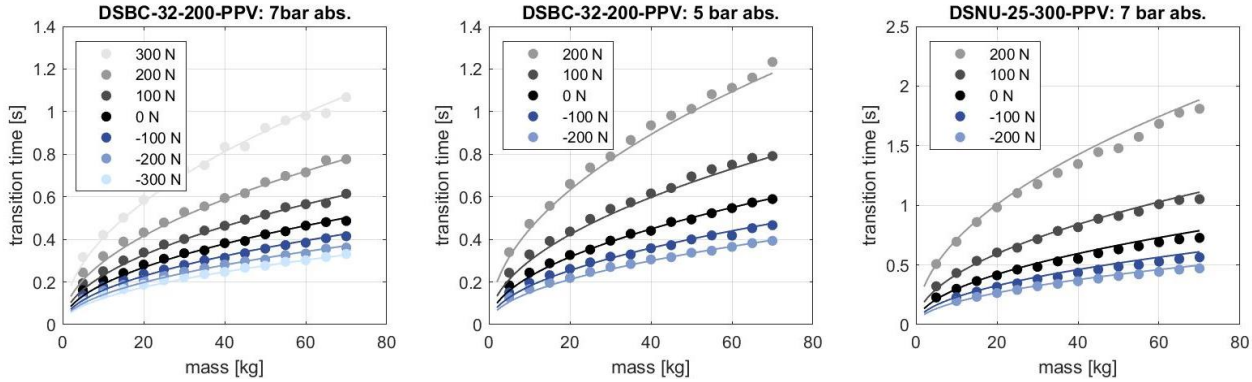

Figure 7: Validation data of the extended PFR for different diameters, lengths, and pressures.

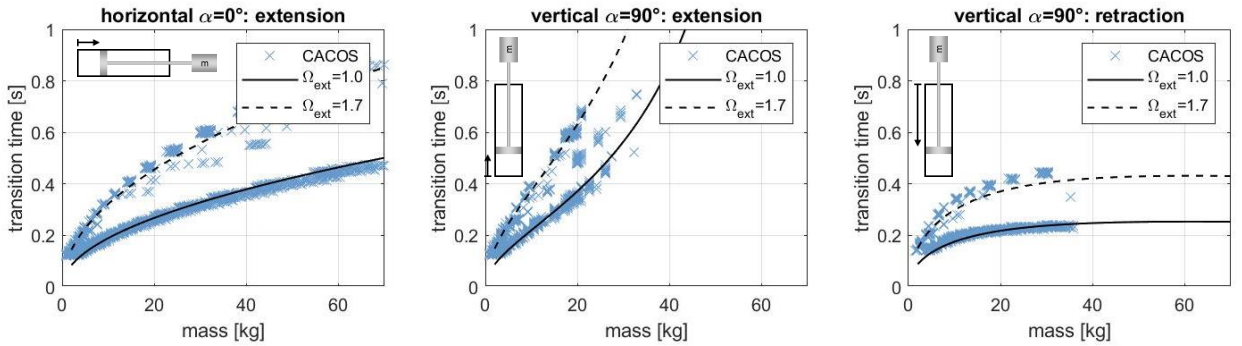

Figure 8: Approximation of the transition time using the extended PFR with external forces for horizontal and vertical orientation of a DSBC-32-200-PPV.

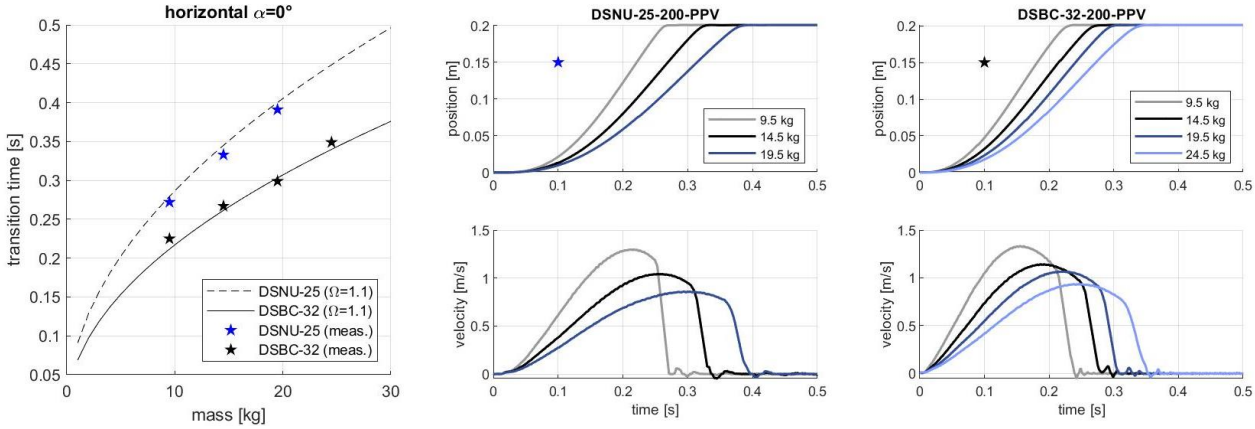

Figure 9: Measurements of two different cylinders with different loads and comparison of the resulting transition times with the PFR approach.

5. VALIDATION AND COMPARISON TO OTHER APPROACHES

In this section we validate the PFR and extended PFR formulas by measurements. Thereby all the measurements were done by adjusting the exhaust flow throttle as well as the throttle of the pneumatic cushioning system, s.th. an optimal behaviour is achieved. That means the fastest possible transition time with the condition of having nearly no oscillation at end stop.

5.1. Validation of PFR

Figure 9 shows the measurements for a horizontal installation position of two systems with several loads in comparison to the calculated transition time of the PFR approach using (4) (same as (10) with F = 0). It shows that for both systems the optimal transition times match quite good the calculation if we use $\Omega = 1.1$ instead of $\Omega = 1.0$. This is a learning from all the measurements done, that in the experiments the PFR is always a little greater than in simulation, and may be caused by idealized conditions within the simulation and mismatches concerning friction forces, pressure losses etc. The curves in principle however match quite good and can be taken for sizing the actuators just by adjusting the PFR.

5.2. Validation of extended PFR

Figure 10 shows the measurement results for a DSBC-32-200-PPV cylinder for the extension stroke in three different orientations ($\alpha = 0°, \alpha = 90°, \alpha = -90°$). Again, for the calculation of the transition times using as (10) and (11) an $\Omega_{ext} = 1.1$ was assumed. As could be seen, the measured transition times match quite good the predicted values of the PFR approach.

5.3. Comparison of the extended PFR to other approaches

In this section we compare the PFR-sizing approach with the constant acceleration and constant velocity approaches for exemplary applications. **Table 1** shows three applications and the corresponding piston diameters by using different approaches.

The **first application** is a typical application which is based on speed. For specifying the required piston diameters two different approaches were used. The first is the constant acceleration approach (acc.) which yields half the diameter as in comparison to the PFR approach. The results of both the systems are shown in **Figure 11** on the left. Thereby using the PFR sizing method yields a reduced velocity at stroke end, whereas a smaller cylinder leads to very high velocities which would indicate an infeasible solution or would lead to the necessity of using external shock absorbers.

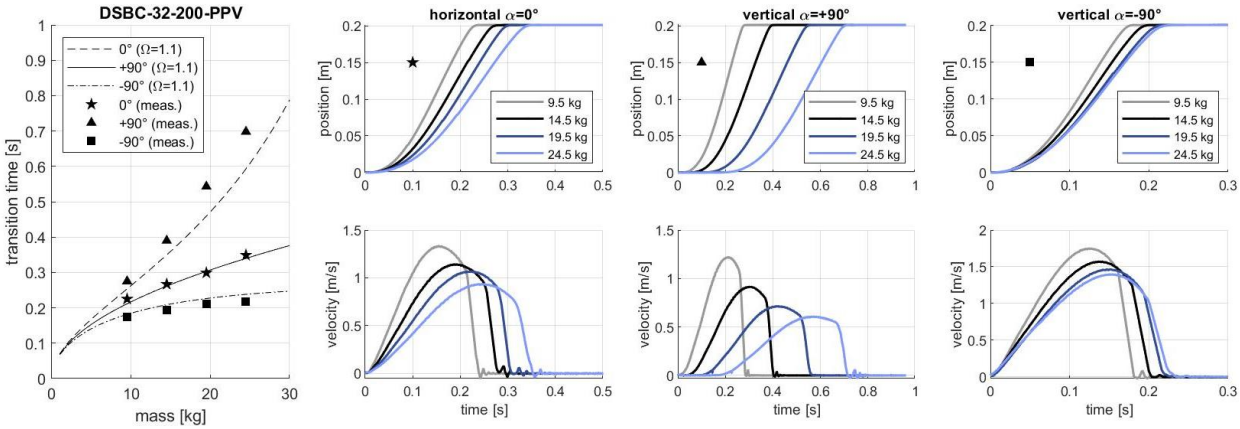

Figure 10: Measurements of a DSBC-32-200-PPV cylinder for the extension stroke in different orientations and comparison of the resulting transition times with the PFR approach for $\Omega_{ext} = 1.1$.

The **second application** is a vertical application with speed requirements. As in application 1, the result is similar, that with the const. acc. and const. vel. approach the cylinder is chosen too small such that a proper motion is not possible. However, when the requirements on the speed are relaxed – as in application 3 - the sizing result is similar.

This is shown in **application 3** which is the same as application 2 but with a very large transition time of $T_f = 7\ s$. As the required dynamics is very low the piston diameter then is mainly influenced by the gravitational and friction forces and thus lead to similar results between both approaches. As could be seen in **Figure 11** on the right, the cylinder needs several seconds before it starts to move. This is caused by the exhaust flow throttle which is adjusted to achieve the large transition time.

Table 1: Applications and calculated/**selected** piston diameters.

		Application 1		Application 2		Application 3	
load [kg]	m	12.5 kg		22.5 kg		22.5 kg	
stroke [mm]	l_z	200 mm		300 mm		300 mm	
transition time [s]	T_f	0.25 s		0.45		7 s	
orientation, dir. [°]	α	0° ext.		90° ext.		90° ext.	
		acc.	PFR	vel.	PFR	vel.	PFR
diameter [mm]	d	13.8 / **16**	30.6 / **32**	22.1 / **32**	39.3 / **40**	22.1 / **25**	21.0 / **25**
corresponding PFR	Ω_{ext}	0.49 / 0.57	1.1 / 1.15	0.15 / 0.73	1.1 / 1.13	2.3 / 5.3	1.1 / 5.3
impact velocity [m/s]	v_e	**1.7**	**0.09**	**0.65**	**0.09**	**0.08**	**0.08**
transition time [s]	T_f	0.26	0.24	0.52	0.42	6.8	6.8

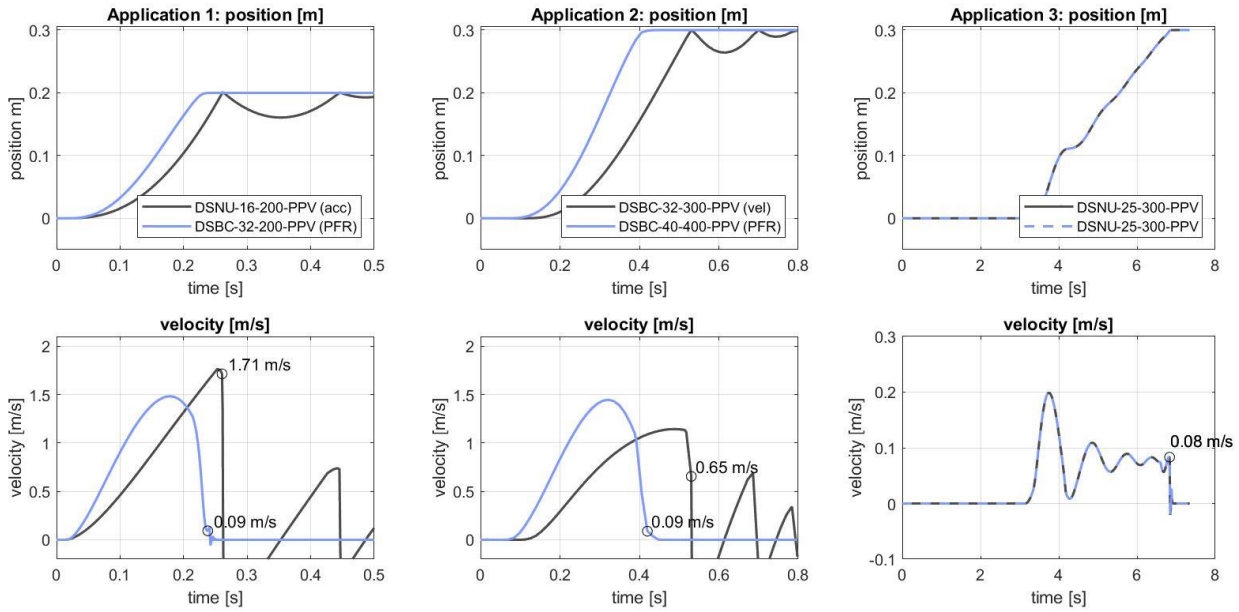

Figure 11: Comparison of different sizing approaches on basis of simulation results for three different applications.

6. CONCLUSIONS

The sizing of the system components is a simple measure to save energy. The choice of piston diameter is crucial here. However, many approaches for sizing only work for short drives or small moving masses because the end position speed is not taken into account or would otherwise lead to greatly oversized drives. In view of an energy-efficient design, however, medium, and large drives play a more important role. For these drives, however, the dynamic behaviour must also be considered, especially in the end position.

The PFR approach takes into account the dynamic properties of the drive and the end position behaviour and can be used for evaluation, design, determination of the transition time or also for calculating a reduced supply pressure for oversized drives. The biggest disadvantage, that the PFR is only valid for a horizontal installation position, was eliminated in this article by a corresponding extension of additional forces. Both approaches of PFR are simple algebraic equations that reflect the essential relationships, but do not represent exact solutions but lead to feasible systems.

In practical applications, the necessary value for Ω can be somewhat larger, as additional pressure drops, dead volumes, hose dynamics or frictional forces from external guides are present. Differences between the two directions of movement are also common due to the different surface ratios. Typical values here are in the range $\Omega \in [1.1, 1.6]$.

Ultimately, the Ω is a design factor that can be determined based on measurements and simulations, so that it can also be used for other cylinders and damping systems.

The presented approach will be used in a future version of the sizing tool of Festo. It has thus reached maturity, so that pneumatics is also equipped for the future in times of climate change.

NOMENCLATURE

A	area	m^2
d	piston diameter (bore size)	m

F	force	N
g	gravitational acceleration	m/s²
L	generalized length	m
l_z	cylinder length	m
l_t	dead length	m
m	mass	kg
p	pressure	Pa
T_f	transition time	s
α	angle of orientation	rad
Ω	pneumatic frequency ratio	-
ext	Index indicating the extension	-

CACOS	Computer Aided Cylinder Optimisation System, a simulation tool of Festo SE & Co. KG
DSBC	Standards-based profile cylinder (ISO 15552) of Festo SE & Co. KG Type code: "DSBC-diameter-length"
DSNU	Round cylinder (ISO 6432) of Festo SE & Co. KG Type code: "DSNU-diameter-length"
PFR	Pneumatic Frequency Ratio
PPV	adjustable pneumatic cushioning system of Festo SE & Co. KG

REFERENCES

[1] https://www.festo.com/x/pneumatic-sizing, Festo SE & Co. KG, 10.01.2024

[2] Boyko V, Nazarov F, Gauchel W, Neumann R, Doll M, Weber J (2024) Comprehensive Application-Based Analysis of Energy-Saving Measures in Pneumatics [Manuscript submitted for publication]. Int. J. of Fluid Power.

[3] Doll M (2016) Optimierungsbasierte Strategien zur Steigerung der Energieeffizienz pneumatischer Antriebe. Shaker Verlag, Aachen

[4] Doll M, Neumann R (2014) How big is the efficiency of pneumatic drives? An experiment provides clarity! 9th IFK, March 24-26

[5] Boyko V, Hülsmann S, Weber J (2021) Comparative analysis of actuator dimensioning methods in pneumatics. Proceedings of the ASME/BATH 2021, Symposium on Fluid Power and Motion Control, FPMC2021; October 19-21, Virtual, Online

[6] Rakova E, and Weber J (2016) Exonomy analysis for the selection of the most cost-effective pneumatic drive solution. Proc. of the 9th FPNI Ph.D. Symposium on Fluid Power. FPNI2016-1518. DOI 10.1115/FPNI2016-1518

[7] Vigolo V, De Negri V. J. (2021) Sizing optimization of pneumatic actuation systems through operating point analysis. J. Dyn. Syst. Meas. Control Vol. 143 No. 5. DOI 10.1115/1.4049170

[8] Doll M, Neumann R, Sawodny O (2015) Dimensioning of pneumatic cylinders for motion tasks, International Journal of Fluid Power 16:1, 11-24 DOI: 10.1080/14399776.2015.1012437

[9] Krytikov G, Strizhak M, Strizhak V (2017) The synthesis of structure and parameters of energy efficient pneumatic actuator, Eastern-European Journal of Enterprise Technologies, 1/7 (85), 38–44. DOI: 10.15587/1729-4061.2017.92833